

Human AICAR Transformylase: Role of the 4-Carboxamide of AICAR in Binding and Catalysis[†]

Mark Wall,[‡] Jae Hoon Shim,[‡] and Stephen J. Benkovic*

Department of Chemistry, 415 Wartik Laboratory, The Pennsylvania State University, University Park, Pennsylvania 16802

Received March 30, 2000; Revised Manuscript Received June 30, 2000

ABSTRACT: We have prepared 4-substituted analogues of 5-aminoimidazole-4-carboxamide ribonucleotide (AICAR) to investigate the specificity and mechanism of AICAR transformylase (AICAR Tfase). Of the nine analogues of AICAR studied, only one analogue, 5-aminoimidazole-4-thiocarboxamide ribonucleotide, was a substrate, and it was converted to 6-mercaptapurine ribonucleotide. The other analogues either did not bind or were competitive inhibitors, the most potent being 5-amino-4-nitroimidazole ribonucleotide with a K_i of $0.7 \pm 0.5 \mu\text{M}$. The results show that the 4-carboxamide of AICAR is essential for catalysis, and it is proposed to assist in mediating proton transfer, catalyzing the reaction by trapping of the addition compound. AICAR analogues where the nitrogen of the 4-carboxamide was derivatized with a methyl or an allylic group did not bind AICAR Tfase, as determined by pre-steady-state burst kinetics; however, these compounds were potent inhibitors of IMP cyclohydrolase (IMP CHase), a second activity of the bifunctional mammalian enzyme ($K_i = 0.05 \pm 0.02 \mu\text{M}$ for 4-*N*-allyl-AICAR). It is proposed that the conformation of the carboxamide moiety required for binding to AICAR Tfase is different than the conformation required for binding to IMP CHase, which is supported by inhibition studies of purine ribonucleotides. It is shown that 5-formyl-AICAR (FAICAR) is a product inhibitor of AICAR Tfase with K_i of $0.4 \pm 0.1 \mu\text{M}$. We have determined the equilibrium constant of the transformylase reaction to be 0.024 ± 0.001 , showing that the reaction strongly favors AICAR and the 10-formyl-folate cofactor. The coupling of the AICAR Tfase and IMP CHase activities on a single polypeptide allows the overall conversion of AICAR to IMP to be favorable by coupling the unfavorable formation of FAICAR with the highly favorable cyclization reaction. The current kinetic studies have also indicated that the release of FAICAR is the rate-limiting step, under steady-state conditions, in the bifunctional enzyme and channeling is not observed between AICAR Tfase and IMP CHase.

The *de novo* purine biosynthetic pathway consists of 10 enzymatic reactions that convert 5-phosphoribosyl-1-pyrophosphate to IMP. This pathway is used by virtually all organisms to produce purine nucleotides that are essential for many cellular processes. Consequently, this pathway has attracted considerable attention for the development of inhibitors, in particular for cancer chemotherapy since rapidly dividing cells require large amounts of purines. The penultimate and final reactions of this pathway are catalyzed by a bifunctional protein with two distinct active sites: 5-aminoimidazole-4-carboxamide ribonucleotide transformylase (AICAR Tfase)¹ and inosine monophosphate cyclohydrolase (IMP CHase). AICAR Tfase catalyzes the transfer of the formyl group from (6*R*,*S*)-10-formyltetrahydrofolate (10-f-H₄F) to AICAR producing 5-formyl-AICAR (FAICAR), which is then subsequently cyclized by IMP CHase to form IMP, Figure 1.

AICAR Tfase is one of two enzymes in the *de novo* purine biosynthetic pathway that use 10-f-H₄F as a cofactor for formyl transfer to an amino group, the other being the more extensively studied third enzyme in the pathway, glycinamide

ribonucleotide transformylase (GAR Tfase). Initially, we thought that the catalytic mechanism of these two enzymes would be similar since the kinetic sequences of both enzymes are sequential, and the catalytic triad of GAR Tfase is also conserved in all species of AICAR Tfase characterized to date. However, Beardsley has shown that mutation of these residues has no effect on the enzyme (1). This result, and a difference of 6 p*K*_a units in the basicity of the amino group of the two substrates (2, 3), led us to question whether the mechanism of AICAR Tfase was different than GAR Tfase. For example, because the 5-amino group of AICAR is such a poor nucleophile, is the formyl group transferred indirectly through a transient formyl–enzyme species, unlike with GAR Tfase where the transfer is direct?

¹ Abbreviations: AICAR, 5-aminoimidazole-4-carboxamide ribonucleotide; AICAR Tfase, AICAR transformylase; IMP CHase, IMP cyclohydrolase; 10-f-H₄F, (6*R*,*S*)-10-formyl-5,6,7,8-tetrahydrofolic acid; 10-f-H₂F, 10-formyl-7,8-dihydrofolic acid; FAICAR, 5-formyl-AICAR; GAR Tfase, glycinamide ribonucleotide transformylase; AIR, 5-amino-1-β-D-ribofuranosylimidazole 5'-phosphate; CAIR, 5-amino-1-β-D-ribofuranosylimidazole-4-carboxylate 5'-phosphate; NAIR, 5-amino-4-nitro-1-β-D-ribofuranosylimidazole 5'-phosphate; AICNR, 5-amino-1-β-D-ribofuranosylimidazole-4-carbonitrile 5'-phosphate; 4-*N*-allyl-AICAR, 5-amino-1-β-D-ribofuranosylimidazole-4-*N*-allylcarboxamide 5'-phosphate; thio-AICAR, 5-amino-1-β-D-ribofuranosylimidazole-4-thiocarboxamide 5'-phosphate; 4-*N*-methyl-AICAR, 5-amino-1-β-D-ribofuranosylimidazole-4-*N*-methylcarboxamide 5'-phosphate; TEAA, triethylammonium acetate.

[†] This work was supported by the National Foundation for Cancer Research and PHS Grant GM24129 from the National Institutes of Health.

* To whom correspondence should be addressed. Phone: 814-865-2882. Fax: 814-865-2973.

[‡] These authors contributed equally to this work.

bicarbonate (3×4 mL). The organic layer was evaporated to dryness and then stirred for 1 h at 25 °C in 1 mL of 50% TFA/H₂O. The solution was evaporated to dryness and purified by reversed-phase HPLC on a Whatman Partisil 10 ODS-3 (9.4 mm \times 50 cm) column, equilibrated in 0.1% TFA, by elution with a linear gradient of 0 to 20% acetonitrile. Appropriate fractions were lyophilized to give 6-mercapto-9- β -D-ribofuranosylpurine 5'-phosphate (11 mg, 50%) as a white solid. ¹H NMR (D₂O): δ 8.40 (s, 1 H, H-2), 7.72 (s, 1 H, H-8), 6.20 (d, 1 H, H-1', $J_{1',2'} = 4.5$ Hz), 4.51 (dd, 1 H, H-3', $J_{3',4'} = 4.4$, $J_{3',2'} = 4.9$), 4.40 (m, 1 H, H-4'), 4.16 (m, 2 H, H-5'). ³¹P NMR (D₂O): δ 0.80. Electrospray MS M-H⁻ m/z 363.

Synthesis of 5-amino-1- β -D-ribofuranosylimidazole-4-*N*-allylcarboxamide 5'-phosphate (4-*N*-allyl AICAR). 5-amino-1-(2',3'-*O*-isopropylidene- β -D-ribofuranosyl)imidazole-4-*N*-allylcarboxamide was prepared in a manner similar to that used by Aoyagi et al. (14) to prepare 5-amino-1- β -D-ribofuranosylimidazole-4-*N*-allylcarboxamide. To a solution of 110 mg (0.33 mmol) of 5-amino-1-(2',3'-*O*-isopropylidene- β -D-ribofuranosyl)imidazole-4-*N*-allylcarboxamide in 2 mL of dichloromethane at 25 °C containing 50 mg (0.75 mmol) of tetrazole was added 135 mg (0.50 mmol) of di-*tert*-butyl diisopropylphosphoramidite. The solution was stirred for 20 min at 25 °C and then cooled to -40 °C, and 83 mg of 3-chloroperoxybenzoic acid was added. After 10 min, the solution was allowed to warm to room temperature and then diluted with 2 mL of dichloromethane and washed with 10% aqueous sodium bicarbonate (2 \times 5 mL) and brine (1 \times 5 mL). The solution was concentrated and purified by elution from a silica gel column with 100% ethyl acetate to give 5-amino-1-(2',3'-*O*-isopropylidene-5-*O*-di-*tert*-butyl phosphate- β -D-ribofuranosyl)imidazole-4-*N*-allylcarboxamide (100 mg, 55%) as a colorless oil. ¹H NMR (CDCl₃): δ 7.17 (s, 1 H, H-1), 7.01 (b, 1 H, NH), 5.84 (ddt, 1 H, CH=CH₂, $J = 17.2$ Hz, $J = 10.2$ Hz, $J = 5.4$ Hz), 5.55 (d, 1 H, H-1', $J = 3.2$ Hz), 5.30 (b, 2 H, NH₂), 5.18 (dd, 1 H, CH=CH_aH_b, $J = 17.2$ Hz, $J = 1.5$ Hz), 5.08 (dd, 1 H, CH=CH_aH_b, $J = 10.2$ Hz, $J = 1.5$ Hz), 5.02 (dd, 1 H, H-3', $J = 6.6$ Hz, $J = 4.1$ Hz), 4.88 (dd, 1 H, H-2', $J = 6.6$ Hz, $J = 3.2$ Hz), 4.27 (m, 1 H, H-4'), 4.18 (ddd, 1 H, H-5'a, $J = 2.5$ Hz, $J = 11.7$ Hz, $J = 6.2$ Hz), 4.08 (ddd, 1 H, H-5'b, $J = 2.7$ Hz, $J = 11.7$ Hz, $J = 5.3$ Hz), 3.94 (m, 2 H, NHCH₂), 1.54 (s, 3 H, CH₃), 1.41 (d, 18 H, *tert*-butyl, $J = 4.6$ Hz), 1.30 (s, 3 H, CH₃). The above compound (50 mg, 0.09 mmol) was deprotected in 1 mL of 50% trifluoroacetic acid for 2 h at 25 °C. The solvent was removed by rotary evaporation, and the residue was taken up in water and lyophilized to give 4-*N*-allyl-AICAR (28 mg, 95%) as white powder. $\lambda_{\max} = 268$ ($\epsilon = 12\,300$) pH 7.5. ¹H NMR (D₂O): δ 8.57 (s, 1 H, H-2), 5.93 (ddt, 1 H, CH=CH₂, $J_{\text{trans}} = 17.3$ Hz, $J_{\text{cis}} = 10.5$ Hz, $J = 5.0$ Hz), 5.87 (d, 1 H, H-1', $J_{1',2'} = 5.1$ Hz), 5.24 (ddt, 1 H, CH=CH_aH_b, $J_{\text{trans}} = 17.3$ Hz, $J_{\text{gem}} = 1.4$ Hz, $J = 1.4$ Hz), 5.19 (ddt, 1 H, CH=CH_aH_b, $J_{\text{cis}} = 10.5$ Hz, $J_{\text{gem}} = 1.4$ Hz, $J = 1.4$ Hz), 4.62 (dd, 1 H, H-2', $J_{2',1'} = J_{2',3'} = 5.0$ Hz), 4.43 (m, 2 H, H-3', H-4'), 4.19 (ddd, 1 H, H-5'a, $J_{5'a,4'} = 1.8$ Hz, $J_{5'a,b} = 11.9$ Hz, $J_{5'a,p} = 4.2$ Hz), 4.11 (ddd, 1 H, H-5'b, $J_{5'b,4'} = 1.8$ Hz, $J_{5'b,b} = 11.9$ Hz, $J_{5'b,p} = 5.0$ Hz), 3.97 (dt, 2 H, NHCH₂, $J = 5.4$ Hz, $J = 1.8$ Hz). ³¹P NMR (D₂O): δ 0.58. Electrospray HRMS 377.0851 (M-H⁻, C₁₂H₁₈N₄O₈P requires 377.0862).

HPLC Purifications. The purity of all compounds was verified by analytical HPLC on a BetaBasic C18 (150 \times 4.6 mm) column by elution with 100% of 10 mM triethylammonium acetate (TEAA) (pH 7) for 4 min followed by a linear gradient of 0 to 40% CH₃CN over 11 min. Compounds were purified, if necessary, by semipreparative reversed-phase HPLC on a Whatman Partisil 10 ODS-3 (9.4 mm \times 50 cm) column with a linear gradient of 0 to 50% acetonitrile in either 0.1% TFA/H₂O or 10 mM TEAA (pH 7). Appropriate fractions were collected and lyophilized.

Protein Preparations. Human bifunctional enzyme was prepared by using a vector that codes a His-tagged human purH cDNA and IPTG induction of the T7 promoter in *Escherichia coli* BL21(DE3). These cells were grown in LB media with 25 μ g/mL kanamycin at 37 °C up to an OD₆₀₀ of 0.5. Protein production was induced by adding IPTG (0.5 mM final concentration), and cells were grown for an additional 4.5 h at 37 °C. Cells were harvested by centrifugation.

Cells were resuspended in a buffer containing 33 mM Tris-Cl and 25 mM KCl, pH 7.5 (buffer A), and lysed by sonication. After centrifugation at 40000g for 1 h, supernatant was loaded onto a 2-mL Ni-NTA agarose column. The column was consecutively washed with 20 mL buffer A containing 150 mM NaCl and 20 mL buffer A containing 150 mM NaCl and 20 mM imidazole. The desired protein was finally eluted with buffer A containing 150 mM NaCl and 250 mM imidazole. The eluted protein was either dialyzed to remove imidazole or loaded onto a 2.5 \times 45 cm Sephadex G-100 column equilibrated in buffer A to further purify the bifunctional enzyme. The purity of the protein was determined on SDS-PAGE. The molecular mass of the purified protein was confirmed by MALDI mass spectrometry to be 66 779 Da.

Kinetic Measurements. All kinetic measurements were performed at 25 °C in buffer A. Enzyme assays were carried out in a 1-mL cuvette thermostated on a Cary spectrophotometer. AICAR Tfase was assayed by following the production of H₄F at 298 nm ($\Delta\epsilon = 19.7$ mM⁻¹ cm⁻¹) or H₂F at 298 nm ($\Delta\epsilon = 18.0$ mM⁻¹ cm⁻¹), and IMP CHase was assayed by following IMP production at 248 nm ($\Delta\epsilon = 5.7$ mM⁻¹ cm⁻¹). When thio-AICAR was a substrate, $\Delta\epsilon$ (298 nm) = 25.3 mM⁻¹ cm⁻¹ was used, which takes into account the contribution from 6-mercapto-purine ribonucleotide. Data from saturation kinetics were fit to the Michaelis-Menten equation to obtain k_{cat} and K_m values. K_i 's were determined from plots of $1/v$ versus $1/[S]$ at several levels of inhibitors. When the K_i values for FAICAR, AMP, or XMP to AICAR Tfase were measured, 120 μ M of 4-*N*-allyl-AICAR was added to inhibit the IMP CHase. The steady-state kinetic parameters of IMP CHase were not accurately measured using the spectrophotometric assay since the K_m for FAICAR was <1 μ M, consistent with the previous reports (1, 15). The K_i values for 4-*N*-allyl-AICAR and 4-*N*-methyl-AICAR were estimated using Dixon plots with K_m value of 0.87 μ M (16).

Stopped-flow experiments for AICAR Tfase activity were performed on an Applied Photophysics Kinetic Spectrometer (Cambridge, England) equipped with a thermostated sample cell. Absorbance measurements were conducted at 298 nm with a 0.5-mm slit width. In the pre-steady-state burst kinetics, the enzyme (2.5 μ M) was preincubated with 10-f-

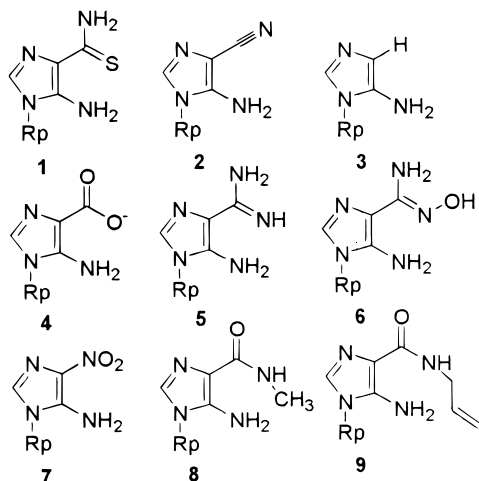


FIGURE 2: Structures of AICAR analogues: 1, thio-AICAR; 2, AICNR; 3, AIR; 4, CAIR; 5, 5-amino-1- β -D-ribofuranosylimidazole-4-carboxamide 5'-phosphate; 6, 5-amino-1- β -D-ribofuranosylimidazole-4-carboxamidoxime 5'-phosphate; 7, NAIR; 8, 4-*N*-methyl-AICAR; 9, 4-*N*-allyl-AICAR. Rp represents β -D-ribofuranosyl 5'-phosphate.

Table 1: Comparison of Steady-State Kinetic Parameters of AICAR and Thio-AICAR Reaction

	k_{cat} (s^{-1})	K_m (μM)	K_m (folate) (μM)
AICAR (10-f-H ₂ F)	4.1 ± 0.3	1.5 ± 0.2	11 ± 1
AICAR (10-f-H ₄ F)	3.7 ± 0.2	1.9 ± 0.4	39 ± 6
thio-AICAR (10-f-H ₂ F)	0.92 ± 0.10	0.9 ± 0.4	32 ± 5

H₂F (120 μM) and reacted with AICAR or thio-AICAR (90 μM). When inhibition by 4-*N*-methyl-AICAR, 4-*N*-allyl-AICAR, or purine monophosphates was examined, these compounds (150–250 μM) were preincubated with the enzyme (2.5 μM) and 10-f-H₂F (120 μM) and reacted with 90 μM of AICAR. In the single turnover experiments, enzyme (14–21 μM) was preincubated with saturating amounts of 10-f-H₂F (160 μM) and reacted with limiting amount of AICAR or AICAR analogues (3.5 μM). In most experiments, 5–8 traces were recorded and averaged for data analysis on an Acorn computer. All data were analyzed by nonlinear least-squares analysis using software provided by Applied Photophysics or transferred to a PC and analyzed using KaleidaGraph.

RESULTS

Characterization of AICAR Analogues. The compounds shown in Figure 2 were tested as substrates for AICAR Tfase by determining their ability to deformylate 10-f-H₂F under single turnover conditions. Baggott and co-workers (11) have shown that 10-f-H₂F is an alternative cofactor for human AICAR Tfase, and since it is more stable than 10-f-H₄F and has a lower K_m , we have used it in our kinetic experiments (Table 1). It is known that AICAR Tfase follows a sequential ordered mechanism with folate binding first to the enzyme (15, 17). In testing AICAR analogues under single turnover conditions, the enzyme was preincubated with 10-f-H₂F to ensure that folate is in the active site when the AICAR analogue binds. Of all the compounds screened, only thio-

Table 2: K_i Values for AICAR Analogs to AICAR Tfase

entry	K_i (μM)
1	0.9 ± 0.4^a
2	26 ± 8
3	6 ± 2
4	10 ± 4
5	nd
6	>50
7	0.7 ± 0.5
8	nd
9	nd

^a K_m value; nd, no inhibition detected.

AICAR was a substrate for AICAR Tfase, the rest were inhibitors, and the results are shown in Table 2. All of these compounds were competitive with AICAR.

Characterization of the Reaction Between Thio-AICAR and 10-f-H₂F Catalyzed by AICAR Tfase-IMP CHase. If the transfer of a formyl group from 10-f-H₂F to thio-AICAR, catalyzed by the bifunctional enzyme, is analogous to the formylation of AICAR, we expect the initial product to be 5-formyl-thio-AICAR, which will be subsequently cyclized to 6-mercaptapurine ribonucleotide. The only product of the reaction that we were able to isolate and characterize was 6-mercaptapurine ribonucleotide. This was identified by comparison of the HPLC retention time and UV-vis spectra with a sample prepared independently by phosphorylation of the commercially available 6-mercaptapurine ribonucleoside. The enzymatically prepared material was also isolated, and mass spectral analysis gave a molecular ion of 363 Da ($[\text{M}-\text{H}]^-$ electrospray MS), which is consistent with the product being 6-mercaptapurine ribonucleotide.

It is important to note that the bifunctional enzyme converts thio-AICAR to 6-mercaptapurine ribonucleotide, an inhibitor of purine biosynthesis used in the treatment of human leukemias [6-mercaptapurine ribonucleotide is an active metabolite of the drug mercaptopurine (18)]. It is unknown whether thio-AICAR would be clinically useful due to the negative charge of the 5'-phosphate; however, it may be possible to form thio-AICAR intracellularly with an appropriate enzyme, such as a kinase or a phosphoribosyl-transferase.

The steady-state kinetic parameters of the thio-AICAR reaction are given in Table 1. The k_{cat} value of formylation of thio-AICAR was about 4 times lower than that for formylation of AICAR. The K_m value for thio-AICAR was very similar to that of AICAR, and the K_m value for 10-f-H₂F was 3-fold higher.

Pre-Steady-State Burst. As shown in Figure 3, the AICAR Tfase reaction using AICAR showed a pre-steady-state burst followed by a steady-state formation of products. The rate constant of the burst (k_{burst}), 30 s^{-1} , was about 10 times higher than the steady-state rate (k_{ss}), and the amplitude is very close to the total concentration of the enzyme used. This indicates that the steady-state k_{cat} value is predominantly determined by a rate-limiting step after chemistry. However, the thio-AICAR reaction did not show a pre-steady-state burst but a steady-state increase of product formation with a rate constant of 0.5 s^{-1} . This rate may represent the rate-limiting chemistry step. Therefore, substitution of oxygen in the carboxamide to sulfur slowed the rate of chemistry by at least a factor of 60. This analysis indicates that the carboxamide moiety may play an important role in the chemistry of formyl transfer.

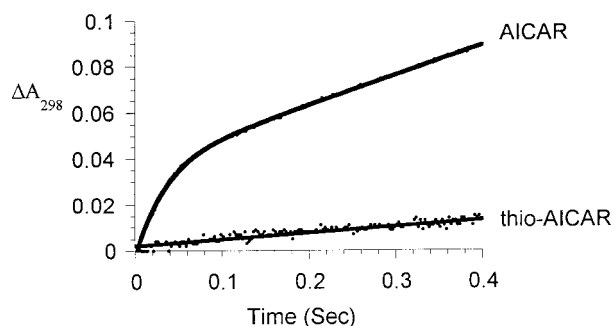


FIGURE 3: Comparison of the pre-steady-state burst of the AICAR reaction with the steady-state product formation of the thio-AICAR reaction. The enzyme (2.5 μM) was preincubated with 10-f-H₂F (250 μM) and reacted with AICAR (90 μM) or thio-AICAR (90 μM) on a stopped-flow instrument. Reactions were monitored at 298 nm. The amplitude of the burst was 2.3 μM , k_{burst} was 30 s^{-1} , and k_{ss} was 2.9 s^{-1} . The k_{ss} for thio-AICAR reaction was 0.5 s^{-1} .

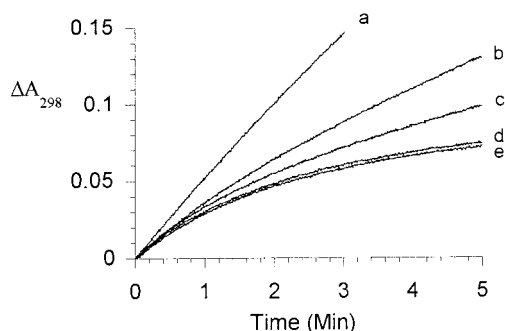


FIGURE 4: Inhibition of AICAR Tfase by 4-*N*-allyl-AICAR. The enzyme (20 nM) was preincubated with 10-f-H₂F (45 μM) and 4-*N*-allyl-AICAR [(a) 0.0, (b) 3.2, (c) 6.5, (d) 65.0, and (e) 130.0 μM] and reacted with AICAR (31 μM). The same curves were obtained when 4-*N*-allyl-AICAR was not preincubated with the enzyme.

N-Substitution in the Amide of AICAR. 4-*N*-allyl-AICAR was not a substrate for AICAR Tfase but showed the characteristics of slow tight binding inhibition in initial velocity measurements (Figure 4). However, the reaction yielded identical curves whether the enzyme was preincubated with 4-*N*-allyl-AICAR or not, indicating that 4-*N*-allyl-AICAR may not act as a slow tight binding inhibitor by itself. Another possibility was that a multiadduct inhibitor was generated in situ, although the 4-*N*-allyl group would be expected to be unreactive under these conditions. As expected, the HPLC chromatogram of the products from the reaction in the presence of 4-*N*-allyl-AICAR revealed no new species formed (data not shown).

Another possibility is that 4-*N*-allyl-AICAR is only inhibiting IMP CHase and FAICAR cannot transfer to IMP CHase but remains in the active site of AICAR Tfase as a strong product inhibitor. For proof of this model, three questions should be addressed: (1) Does 4-*N*-allyl-AICAR inhibit IMP CHase? (2) Does FAICAR give strong product inhibition of AICAR Tfase? (3) Does 4-*N*-allyl-AICAR inhibit only IMP CHase and not AICAR Tfase?

To answer the first question, IMP CHase activity was measured using FAICAR in the presence of 4-*N*-allyl-AICAR. IMP CHase was strongly inhibited by 4-*N*-allyl-AICAR, and the K_i value was estimated to be 0.05 ± 0.02 μM . For the second question, a small amount of FAICAR (12 μM) was added to a reaction that contained excess AICAR (64 μM), and the reaction profile was examined as

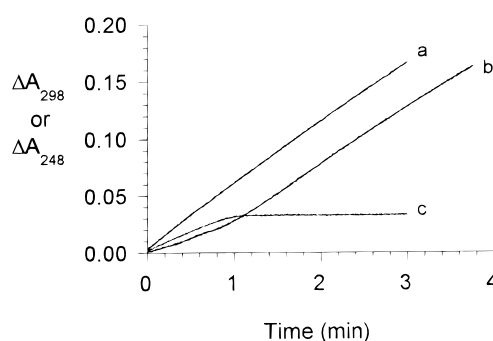


FIGURE 5: AICAR Tfase reaction in the presence of FAICAR. (a) Control reaction (ΔA_{298}) using 20 nM enzyme, 48 μM 10-f-H₂F, and 64 μM AICAR. (b) Control reaction plus FAICAR (12 μM) (ΔA_{298}). (c) IMP CHase reaction (ΔA_{248}) using 12 μM FAICAR.

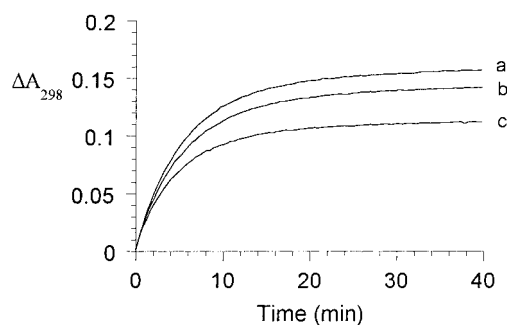


FIGURE 6: Reactions of the formylation of AICAR by 10-f-H₂F in AICAR Tfase reach equilibria when IMP CHase is blocked by 4-*N*-allyl AICAR. AICAR Tfase reaction using 20 nM enzyme in the presence of 4-*N*-allyl-AICAR (246 μM) and (a) 48 μM 10-f-H₂F and 92 μM AICAR, (b) 72 μM 10-f-H₂F and 46 μM AICAR, and (c) 48 μM 10-f-H₂F and 46 μM AICAR.

a function of time (Figure 5). Initially, the reaction is about 4 times slower than the control, showing that FAICAR is inhibiting AICAR Tfase. After about 1 min, the rate recovers very close to that of the control reaction. A separate experiment showed that the same amount of FAICAR was completely turned over by IMP CHase within 1 min (Figure 5). Thus, only after FAICAR is consumed by IMP CHase does AICAR Tfase recover its full activity. The K_i value of FAICAR to AICAR Tfase was estimated to be 0.4 ± 0.1 μM , determined in the presence of 4-*N*-allyl-AICAR to block the IMP CHase active site. However, this K_i value could not explain the activity curves in Figure 4 that appeared to level off at high concentrations of 4-*N*-allyl AICAR. For example, the ratio of [E-FAICAR] to [E-AICAR] after 5 min (slope ~ 0) in the curve of 120 μM 4-*N*-allyl AICAR was calculated to be about 3.6:6.4 (using [FAICAR] at 5 min = 4 μM and assuming that the K_d for AICAR = K_m and that the binding affinities of both folate species are equal and independent of the binding of AICAR or FAICAR). This strongly suggests that the AICAR Tfase reaction reaches an equilibrium favoring starting materials when IMP CHase activity is completely inhibited. This was confirmed by running reactions using different concentrations of AICAR or 10-f-H₂F while inhibiting IMP CHase with 4-*N*-allyl AICAR (Figure 6). Reactions reached equilibria at different levels depending on the amount of starting material providing a value for K_{eq} of 0.024 ± 0.001 .

However, these results still do not give any indication of whether 4-*N*-allyl-AICAR actually inhibits AICAR Tfase or not. To resolve this matter, we examined the pre-steady-

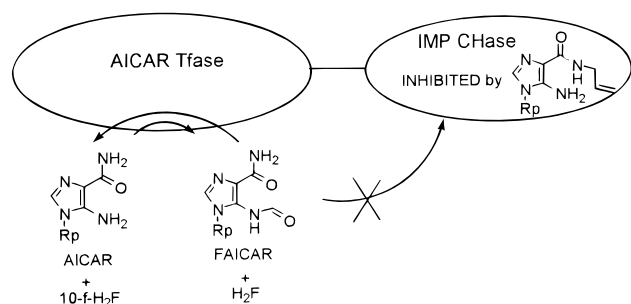


FIGURE 7: Model to explain the 4-*N*-allyl-AICAR and 4-*N*-methyl-AICAR inhibition of AICAR Tfase. In this model, 4-*N*-allyl-AICAR or 4-*N*-methyl-AICAR inhibits only IMP CHase, and FAICAR produced in AICAR Tfase cannot transfer to IMP CHase but is in equilibrium with the starting materials.

Table 3: Burst Kinetic Parameters for Substrate Analogues and Purine Monophosphates^a

	amplitude (μM)	k_{burst} (s^{-1})	k_{ss} (s^{-1})
control	2.27 ± 0.01	30.0 ± 0.3	2.88 ± 0.01
4- <i>N</i> -allyl-AICAR	2.35 ± 0.01	31.1 ± 0.4	2.68 ± 0.01
4- <i>N</i> -methyl-AICAR	2.59 ± 0.02	29.2 ± 0.3	2.91 ± 0.01
IMP	2.29 ± 0.02	28.4 ± 0.3	3.22 ± 0.01
AMP	1.75 ± 0.01	28.9 ± 0.3	2.09 ± 0.01
XMP	1.07 ± 0.01	26.9 ± 0.5	1.32 ± 0.01
GMP	2.62 ± 0.02	28.7 ± 0.3	3.03 ± 0.01

^a These parameters were determined using 200 μM of inhibitors except 150 μM for XMP.

state burst kinetics of AICAR Tfase in the presence of 4-*N*-allyl-AICAR. It is expected that inhibition of AICAR Tfase by 4-*N*-allyl-AICAR would lower the amplitude and k_{ss} values but not the k_{burst} value. In this experiment, the enzyme was preincubated with 10-f-H₂F and 4-*N*-allyl-AICAR to ensure that an inhibitory complex has sufficient time to form. However, the reaction showed virtually no change in the pre-steady-state burst parameters from those of the control, indicating that 4-*N*-allyl-AICAR has no apparent binding to the active site of AICAR Tfase. Our rationale for the effect of 4-*N*-allyl-AICAR on AICAR Tfase and IMP CHase activities is shown in Figure 7.

Interestingly, 4-*N*-methyl-AICAR showed the same kinetic behavior as 4-*N*-allyl-AICAR, although the degree of inhibition is less than that of 4-*N*-allyl-AICAR. Like 4-*N*-allyl-AICAR, it only inhibits IMP CHase and does not cause any change in the burst kinetics of AICAR Tfase. The K_i value for *N*-methyl-AICAR to IMP CHase was estimated to be $1.36 \pm 0.35 \mu\text{M}$.

Inhibition by Purine Ribonucleotides. Several purine ribonucleotides were tested for inhibition of AICAR Tfase. As they are known inhibitors of IMP CHase (19), their inhibition of AICAR Tfase was examined by their effect on the pre-steady-state burst kinetics of AICAR Tfase, using the same procedure as for 4-*N*-allyl-AICAR (Table 3). Of the four purine ribonucleotides tested, only AMP and XMP decreased the amplitude and k_{ss} values from those of the control. The K_i values for AMP and XMP to AICAR Tfase were estimated to be 27 ± 3 and $1.2 \pm 0.4 \mu\text{M}$, respectively.

DISCUSSION

As part of a research program designed to investigate the mechanism of AICAR Tfase, we have determined the

properties of several 4-substituted AICAR derivatives. Initially, we had expected that some of these analogues would be substrates for the enzyme; however, it became apparent that a carboxamide or thiocarboxamide was essential for formyl transfer to occur. Of the nine 4-substituted AICAR analogues we prepared, only thio-AICAR was a substrate, being converted to 6-mercaptapurine ribonucleotide, and the remaining compounds were inhibitors or did not bind to the enzyme. However, it is possible that the analogues were formylated but the products were short-lived and reversed back to starting materials, resulting in no appreciable AICAR Tfase activity. In fact, the formylation of AICAR by 10-f-H₂F is reversible with an equilibrium constant of 0.024 ± 0.001 , favoring starting materials. Despite this low K_{eq} , we were able to observe significant accumulation of FAICAR spectrophotometrically (Figure 4). Therefore, it is necessary that the equilibrium constant for formylation of the analogues not be significantly lower than that for formylation of AICAR to observe formylation of these analogues. Because the equilibrium constants for formamide formation are anticipated to be dependent on the $\text{p}K_{\text{a}}$ value of the 5-amino group, the analogues in this study, with the possible exception of NAIR, have $\text{p}K_{\text{a}}$'s that are similar to or greater than the $\text{p}K_{\text{a}}$ of the 5-amino group of AICAR. In addition, the formylated analogues are stable since these compounds or their aglycon, with the exception of CAIR, have been reported (20–27). Consequently, we should have observed formylation of these analogue if they functioned as substrates.

If the formyl group is not transferred directly to the 5-amino group but via an enzyme intermediate, we expected that these inhibitors might initiate deformylation of the folate cofactor. However, we did not observe any deformylation of 10-f-H₂F as examined under single turnover conditions, suggesting that the formyl transfer is direct, consistent with earlier work (15). The properties of these analogues lead us to propose a role for the 4-carboxamide of AICAR in formyl transfer.

Conformation of the 4-Carboxamide Moiety in the AICAR Tfase Site. The two AICAR analogues substituted on the nitrogen of the 4-carboxamide group with a methyl (8) or allyl (9) group gave interesting AICAR Tfase inhibition curves (Figure 4), which, initially we thought were characteristic of slow tight binding inhibition. However, it became apparent that these analogues were inhibitors of IMP CHase, causing FAICAR to accumulate and that we were observing the transformylase reaction proceeding to equilibrium. Further analysis with burst kinetics showed that neither 4-*N*-substituted analogue bound to AICAR Tfase, only to IMP CHase. We propose that the reason these inhibitors bind only to IMP CHase is that the carboxamide group of the substrates is in a different conformation in each active site. In IMP CHase, the carboxamide of FAICAR must be oriented as shown in Figure 8B for cyclization to occur, and analogues 8 and 9 are likely to be good inhibitors because the 4-*N*-substituents can occupy the formyl binding pocket of FAICAR (Figure 8C). However, we propose that substrates in the AICAR Tfase site bind with the carboxamide rotated 180° (Figure 8A) so that the *N*-substituents of 8 and 9 cannot occupy the formyl binding pocket without steric interactions that prevent binding. This conformation, with the carboxamide nitrogen *cis* to the imidazole N-3, is the one that is observed in the crystal structure of AICAR (28), although

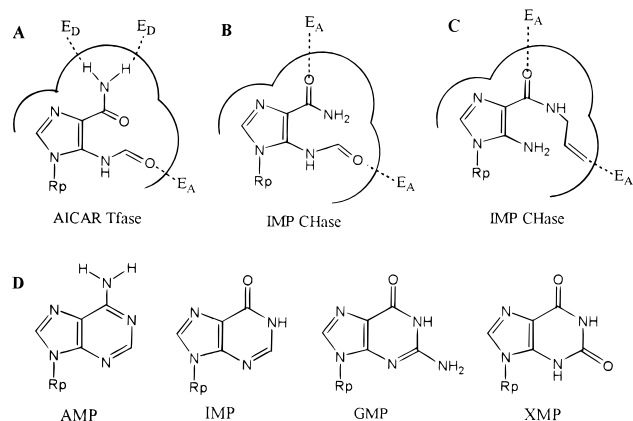


FIGURE 8: Conformation of (A) FAICAR in AICAR Tfase active site; (B) FAICAR in IMP CHase active site; (C) 4-N-Allyl-AICAR in IMP CHase active site; and (D) Structure of purine ribonucleotides. E_A and E_D represent hydrogen bonding acceptor and donor, respectively.

as of yet there is no structural evidence to support this conformation in the active site of AICAR Tfase.

For further data to support the conformation of the carboxamide in each active site, we investigated the properties of several purine ribonucleotides that can mimic both conformations of the carboxamide. If the conformation of the carboxamide in the AICAR Tfase active site is as shown in Figure 8A, then AMP should inhibit AICAR Tfase, and if the opposite conformation is required for binding we would predict that IMP is a better inhibitor. Our kinetic results clearly show that AMP inhibits AICAR Tfase as indicated by a decrease in both amplitude and k_{ss} in the burst kinetics, while IMP or GMP up to 250 μ M showed no such decreases. However, XMP also inhibited AICAR Tfase even though its amide conformation is opposite to that of the predicted structure. The binding affinity of XMP to AICAR Tfase is most likely due to the carbonyl group at C-2 that resembles the formyl group of FAICAR, which has a 2 order of magnitude higher binding affinity to AICAR Tfase than AICAR. Therefore, the conformation of the amide moiety and the presence of the formyl group must be the key determinants in binding of the substrates to AICAR Tfase.

Role of Carboxamide in Formyl Transfer. It is possible that the sole function of the carboxamide is to organize the active site, through binding interactions, in such a way that is essential for formyl transfer to occur. The only analogue that was accepted as a substrate for the enzyme was thio-AICAR and the rate of formylation of this compound was 60-fold lower. This could be a steric effect since sulfur is larger than oxygen and will cause slight perturbations in the active site that could reduce the rate. However, AIR, which lacks the 4-carboxamide, binds with an affinity similar to AICAR, but is not formylated, suggesting that the essential nature of the carboxamide is not solely a binding determinant.

Most reactions involving the addition of an amine to a carbonyl are subject to general acid–base catalysis, and the formylation of AICAR, in particular, is expected to require such catalysis. This is because AICAR, being a very weak base [pK_a of 5-amino group of AICA-riboside is 2.4 (2)], will be rapidly expelled from the addition intermediate, and trapping of this species by proton-transfer becomes necessary (29). The crystal structure of AICAR shows a strong

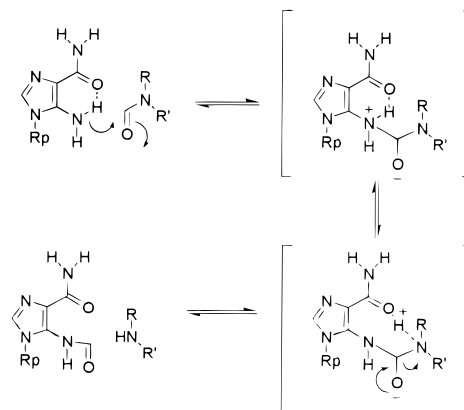


FIGURE 9: Proposed mechanism of AICAR Tfase. Direct attack of the amino group gives an addition compound that is trapped via proton transfer to the carboxamide, followed by breakdown to give products. It is not known whether the protonated amide species exists as an intermediate or if it is only present transiently.

hydrogen bond between the amide carbonyl and the 5-amino group, and based on the inhibition of AICAR analogues **8** and **9** and of AMP and IMP, this conformation is most likely the one in the AICAR Tfase active site. This hydrogen bond orients the amide such that it is positioned to act as a shuttle to assist in proton transfer from the attacking amino group, Figure 9. In an aqueous, nonenzymic reaction, catalysis of proton transfer involving a carboxamide group is unlikely to be observed because the pK_a for protonation of an amide is comparable to water. However, in an enzyme active site where the concentration of water may be low, it may be possible to observe catalysis by weak bases. It is not known whether the protonated amide species exists as a discrete intermediate or if it is only present transiently as the proton is transferred to another group such as the leaving group nitrogen, water, or an active site residue. We are presently performing calculations to explore these possibilities.

The hypothesis of the amide functioning as a locus for a proton shuttle is also consistent with the 60-fold reduction in the rate of chemistry when the carboxamide is replaced with a thiocarboxamide. A thiocarboxamide is a weaker hydrogen bonding base than a carboxamide and therefore would be less efficient as a proton shuttle. One would also predict that NAIR would not be a substrate since a nitro group cannot function as a general base. The pK_a for protonation of nitrobenzene is -11 , 10 orders of magnitude lower than the pK_a for protonation of benzamide (30).

In support of this theory, we wanted to prepare analogues with groups that could transfer the proton in a similar manner. We prepared CAIR and the amidine derivative **5**, compounds with basic moieties in the 4-position of AICAR. However, both of these compounds failed to act as substrates. For CAIR, this may be due to the negative charge of the carboxylate that leads to reduction of the binding affinity and nonproductive binding of this analogue. The K_i of CAIR is 5 times the K_m of AICAR. The amidine of **5**, however, is too basic (pK_a 12), and it exists in the protonated form and does not bind to the enzyme.

On the basis of these investigations, we propose a catalytic mechanism for AICAR Tfase as shown in Figure 9. Earlier work indicated that the amino group of AICAR directly attacks the formyl group of folate. The carboxamide functions as a general base catalyst to trap the addition intermediate

by removal of the proton of the N-5 amino group. It is likely that the carboxamide mediates proton transfer to the nitrogen of the leaving group in a proton shuttle mechanism. In GAR Tfase, an active site residue (Asp144) performs this task (31). This activation alone does not explain the observed catalytic rate of AICAR Tfase. As our work has been focused on substrate analogues, so far we have no evidence of catalysis involving activation of the formyl group of folate. An X-ray crystal structure of AICAR Tfase complexed with substrates would be useful to investigate detailed catalytic events involving amino acid residues in the active site.

Transport of FAICAR in the Bifunctional Enzyme. The pre-steady-state burst indicated that the rate-limiting step of the AICAR Tfase reaction should occur after the catalytic step. Our kinetic analysis showed that formyl transfer is reversible, highly favoring 10-formyl-folate and AICAR with a K_{eq} of 0.024 ± 0.001 . Since the V of IMP CHase is known to be about 36 times greater than V of AICAR Tfase (16), it appears that FAICAR release is the rate-limiting step in the bifunctional enzyme under steady-state conditions. This may illustrate the importance of locating the two enzymes in a single polypeptide for an efficient metabolic flux. In fact, the covalent link of two sequential functions has raised a question of channeling of FAICAR between the two enzymes (1, 15). However, Figure 5 shows that exogenous FAICAR preferentially acts as an inhibitor of AICAR Tfase or a substrate of IMP CHase, indicating that substrate channeling is not absolute. Our result is consistent with a recent study that showed that an inclusion of unlabeled FAICAR in the bifunctional enzyme reaction that uses [3 H]-AICAR resulted in a reduction of the amount of [3 H]-IMP formed (16). The fact that inhibitors for IMP CHase such as 4-*N*-allyl AICAR did not cause any change in AICAR Tfase kinetics indicates there may be no communication between two enzyme domains. Recently, Beardsley and his colleagues constructed truncation mutants of the bifunctional enzyme and were able to separate two domains with fully active IMP CHase on the N-terminal end (amino acid residues 1–198) and fully active AICAR Tfase on the C-terminal end (amino acid residues 199–591) (1). Collectively, the bifunctional enzyme is most likely arranged as two structurally and functionally independent domains. With the V/K of IMP CHase also being 36 times that of AICAR Tfase, the proximity of the two enzymes should be sufficient for capture of FAICAR by IMP CHase without channeling or domain–domain communication. However, the proximity of IMP CHase to AICAR Tfase is absolutely necessary for efficient metabolic flux since it makes the overall reaction favorable by coupling the unfavorable formation of FAICAR with highly favorable cyclization reaction. This may be why evolution has kept AICAR Tfase and IMP CHase as a single polypeptide in de novo purine biosynthesis in all species characterized to date from *E. coli* to humans.

It is interesting that AIR and CAIR, substrates for the de novo purine biosynthetic enzymes AIR carboxylase and 5-aminoimidazole-4-(*N*-succinylcarboxamide) ribonucleotide synthetase, respectively, are good inhibitors of AICAR Tfase. It seems unlikely that these compounds will be present free in solution, and their levels are likely to be regulated. One possible mechanism for regulation is the formation of a multiprotein complex where the substrates are sequestered and channeled between enzymes. The existence of such a

complex in the purine biosynthetic pathway has been previously postulated based on kinetic and structural evidence (32–34).

ACKNOWLEDGMENT

We gratefully acknowledge Joe Ramcharan for providing us with the plasmid containing His-tagged bifunctional cDNA. We thank Steve Baker for phosphorylation of NAI-riboside.

REFERENCES

1. Rayl, E. A., Moroson, B. A., and Beardsley, G. P. (1996) *J. Biol. Chem.* 271, 2225–2233.
2. Yamazaki, A., and Okutsu, M. (1978) *J. Heterocyclic Chem.* 15, 353–358.
3. Hartman, S. C., Levenberg, B., and Buchanan, J. M. (1956) *J. Biol. Chem.* 221, 1057–1070.
4. Sugita, T., Aya, H., Ueno, M., Ishizuka, T., and Kawashima, K. (1997) *J. Biochem. (Tokyo)* 122, 309–313.
5. Firestine, S. M., and Davisson, V. J. (1994) *Biochemistry* 33, 11917–11926.
6. Flaks, J. G., Erwin, M. J., and Buchanan, J. M. (1957) *J. Biol. Chem.* 229, 603–612.
7. Firestine, S. M., and Davisson, V. J. (1993) *J. Med. Chem.* 36, 3484–3486.
8. Greenhalgh, M., Shaw, G., Wilson, D. V., and Cusack, N. J. (1969) *J. Chem. Soc. (C)* 2198–2200.
9. Stevens, M. A., Smith, H. W., and Brown, G. B. (1959) *J. Am. Chem. Soc.* 81, 1734–1738.
10. Rowe, P. B. (1971) *Methods Enzymol.* 18B, 733.
11. Baggott, J. E., Johannning, G. L., Branham, K. E., Prince, C. W., Morgan, S. L., Eto, I., and Vaughn, W. H. (1995) *Biochem. J.* 308 (Pt 3), 1031–1036.
12. Yamazaki, A., Kumashiro, I., Takenishi, T., and Ikehara, M. (1968) *Chem. Pharm. Bull.* 16, 2172–2181.
13. Burrows, I. E., and Shaw, G. (1967) *J. Chem. Soc. [Perkin 1]* 11, 1088–1093.
14. Aoyagi, M., Minakawa, N., and Matsuda, A. (1993) *Tetrahedron Lett.* 34, 103–106.
15. Mueller, W. T., and Benkovic, S. J. (1981) *Biochemistry* 20, 337–344.
16. Szabados, E., and Christopherson, R. I. (1998) *Int. J. Biochem. Cell Biol.* 30, 933–942.
17. Beardsley, G. P., Rayl, E. A., Gunn, K., Moroson, B. A., Seow, H., Anderson, K. S., Vergis, J., Fleming, K., Worland, S., Condon, B., and Davies, J. (1998) *Adv. Exp. Med. Biol.* 431, 221–226.
18. Elion, G. B. and Hitchings, G. H. (1965) *Adv. Chemother.* 2, 91.
19. Szabados, E., Hindmarsh, E. J., Phillips, L., Duggleby, R. G., and Christopherson, R. I. (1994) *Biochemistry* 33, 14237–14245.
20. Groziak, M. P., Huan, Z. W., Ding, H., Meng, Z., Stevens, W. C., and Robinson, P. D. (1997) *J. Med. Chem.* 40, 3336–3345.
21. Montgomery, J. A., and Thomas, H. J. (1972) *J. Med. Chem.* 15, 182–187.
22. Parkin, A., and Harrington, P. J. (1982) *J. Heterocyclic Chem.* 19, 33–40.
23. Townsend, L. (1968) *Syn. Proc. Nucleic Acid Chem.* 2, 267.
24. Schubert, V. H., and Heydenhauss, D. (1963) *J. Praktische Chem.* 22, 304–313.
25. Brown, D. J., and Ford, P. W. (1969) *J. Chem. Soc. (C)* 2620–2623.
26. Kadir, K., and Shaw, G. (1980) *J. Chem. Soc., Perkins Trans. 1* 2728–2731.
27. Yamazaki, A., Furukawa, T., Akiyama, M., Okutsu, M., Kumashiro, I., and Ikehara, M. (1973) *Chem. Pharm. Bull.* 21, 692–696.
28. Adamiak, D. A. and Saenger, W. (1979) *Acta Crystallogr. B* 35, 924–928.

29. Jencks, W. P. (1980) *Acc. Chem. Res.* 13, 161–169.
30. Arnett, E. M. (1963) *Prog. Phys. Org. Chem.* 1, 223–403.
31. Shim, J. H., and Benkovic, S. J. (1999) *Biochemistry* 38, 10024–10031.
32. Smith, G. K., Mueller, W. T., Wasserman, G. F., Taylor, W. D., and Benkovic, S. J. (1980) *Biochemistry* 19, 4313–4321.
33. Rudolph, J., and Stubbe, J. (1995) *Biochemistry* 34, 2241–2250.
34. Li, C., Kappock, T. J., Stubbe, J., Weaver, T. M., and Ealick, S. E. (1999) *Struct. Fold. Des.* 7, 1155–1166.

BI0007268